Chapter 4

A fully discrete method based on cubic splines for time-fractional reaction-diffusion equations with smooth and non-smooth solutions [3]

In this chapter, we consider the following time-fractional reaction-diffusion equation (TFRDE)

$$\left({}_0^C D_t^\alpha + \mathscr{L}\right) v(x,t) = F(x,t), \quad (x,t) \in \Omega := (0,b) \times (0,T], \tag{4.1}$$

with initial and boundary conditions

$$\begin{cases} v(x,0) = g(x), & x \in [0,b], \\ v(0,t) = 0, & t \in (0,T], \\ v(b,t) = 0, & t \in (0,T], \end{cases} \tag{4.2}$$

where $0 < \alpha < 1$, $F \in C(\bar{\Omega})$, $g(x) \in C[0,b]$, $\mathscr{L} = -\mu_d \frac{\partial^2}{\partial x^2} + q(t)$ with $\mu_d > 0$ the diffusion coefficient, $q(t) \in C[0,T]$, and $q \geq 0$. Here, ${}_0^C D_t^\alpha$ denotes the Caputo fractional differential operator defined in equation (1.14). The existence and uniqueness of the solution of problem (4.1)-(4.2) have been discussed in [73, 103]. It is worth noting that near the initial time $t = 0$, the solution to problem (4.1)-(4.2) has an

[3]This chapter contains material published in *Journal of Computational and Applied Mathematics*, 434, 115338, 2023, doi: `https://doi.org/10.1016/j.cam.2023.115338`.

initial layer, and the derivative of the solution satisfies the following bound [103]

$$\left|\frac{\partial v}{\partial t}(x,t)\right| \leq c(1+t^{\alpha-1}), \quad \text{for all } t \in (0,T]. \tag{4.3}$$

It is evident from equation (4.3) that the derivative of the solution with respect to time blows up as $t \to 0^+$. So, the formulation of numerical schemes for solving such TFRDEs encounters serious practical and theoretical problems. Therefore, formulating and analyzing suitable numerical methods for problem (4.1)-(4.2) is a difficult and challenging task.

Several authors, such as [35, 36, 47, 72, 109], have discretized the TFRDE on uniform meshes. In these papers, the reaction term is considered to be constant. Further, they have ignored the layer at $t = 0$ and discussed convergence analyses under the assumption that v is smooth on the closed domain $[0, b] \times [0, T]$. So, the numerical methods proposed in these papers cannot produce optimal convergence in the temporal direction for non-smooth data. Therefore, to overcome this difficulty and improve the performance of the numerical methods, time graded meshes were considered [103]. The authors used the central difference scheme in spatial direction and proved convergence of the numerical method.

The main objective of this chapter is to develop and analyze a new fully discrete numerical method to solve problem (4.1)-(4.2) with smooth and non-smooth solutions. The numerical method combines the L1 scheme on a uniform or graded mesh to discretize in time and a cubic spline difference scheme on a uniform mesh to discretize in space. A graded mesh in time is considered to resolve the initial layer at $t = 0$. The stability and convergence analysis of the method for both the smooth and non-smooth solutions are given separately.

The outlines of the present chapter are as follows. In Section 4.1, the regularity of the solution of the considered problem is discussed. In Section 4.2, a fully discrete numerical scheme solving problem (4.1)-(4.2) is developed. Stability and convergence analysis of the scheme for both smooth as well as non-smooth solutions have been established separately in Section 4.3. Further, the numerical results of the proposed numerical method are discussed in Section 4.4 with the help of two test problems. Finally, Section 4.5 concludes the chapter.

4.1 Regular behaviour of the solution

In this section regularity of the solution will be discussed. First, to obtain bounds on the derivatives of the solution to the considered problem, we provide some definitions.

Definition 4.1. The fractional power $\mathscr{L}^{\nu}$ of the operator $\mathscr{L}$ is defined following [40]:

$$D(\mathscr{L}^{\nu}) = \left\{\psi \in L_2(0,b) : \sum_{k=1}^{\infty} \tilde{\lambda}_k^{2\nu} |(\psi, \phi_k)|^2 < \infty\right\}, \quad \forall \nu \in \mathbb{R},$$

here $\{(\tilde{\lambda}_k, \phi_k) : k = 1, 2, \ldots\}$ denote the eigenvalues and eigenfunctions for the Sturm-Liouville two-point boundary value problem

$$\mathscr{L}\phi_k = -\mu_d \phi_k'' + q\phi_k = \tilde{\lambda}_k \phi_k \quad \textit{on } (0,b) \textit{ with } \phi_k(0) = \phi_k(b) = 0.$$

Definition 4.2. If $\psi \in D(\mathscr{L}^{\frac{1}{2}})$, then

$$\|\psi\|_{\mathscr{L}^{\nu}} = \left(\sum_{k=1}^{\infty} \tilde{\lambda}_k^{2\nu} |(\psi, \phi_k)|^2\right)^{1/2}.$$

Theorem 4.1. *For each* $t \in (0,T]$, *let us assume that* $g \in D(\mathscr{L}^{\frac{5}{2}})$, $F(.,t) \in D(\mathscr{L}^{\frac{5}{2}})$, $F_t(.,t)$ *and* $F_{tt}(.,t)$ *are in* $D(\mathscr{L}^{\frac{1}{2}})$ *with*

$$\|F(.,t)\|_{\mathscr{L}^{\frac{5}{2}}} + \|F_t(.,t)\|_{\mathscr{L}^{\frac{1}{2}}} + t^{\varsigma}\|F_{tt}(.,t)\|_{\mathscr{L}^{\frac{1}{2}}} \leq \hat{C},$$

for some constant $\varsigma < 1$, *where* $\hat{C}$ *is a constant independent of* t. *Then, problem (4.1)-(4.2) has a unique solution such that*

$$\begin{aligned} \left|\frac{\partial^l v}{\partial x^l}(x,t)\right| &\leq c, \quad for \;\; 0 \leq l \leq 4, \\ \left|\frac{\partial^l v}{\partial t^l}(x,t)\right| &\leq c(1+t^{\alpha-l}), \quad for \;\; 0 \leq l \leq 2, \end{aligned}$$

where c *is a constant.*

Proof. See [103] for proof. □

4.2 Fully discrete numerical scheme

In this section we will obtain the fully discrete numerical scheme approximating problem (4.1)-(4.2).

4.2.1 Discretization of Caputo derivative on non-uniform meshes

Let N_t be an positive integer. We divide the interval $[0,T]$ into N_t subintervals with $0 = t_0 < t_1 < \cdots < t_{N_t} = T$, $\Delta t_n = t_n - t_{n-1}$ for $1 \leq n \leq N_t$, where

$$t_n = T\left(\frac{n}{N_t}\right)^{\theta}, \quad 0 \leq n \leq N_t. \tag{4.4}$$

Here, $\theta \geq 1$ is the constant mesh grading. For $\theta = 1$, we will have a uniform mesh.

Caputo fractional time derivative defined in (1.14) is approximated using the L1 method at $t = t_n$, for $1 \leq n \leq N_t$, as follows

$$\begin{aligned}
{}_0^C D_t^\alpha v(x,t_n) &= \frac{1}{\Gamma(1-\alpha)} \int_0^{t_n} (t_n - s)^{-\alpha} \frac{\partial v}{\partial s}(x,s) ds, \\
&= \frac{1}{\Gamma(1-\alpha)} \sum_{k=0}^{n-1} \int_{t_k}^{t_{k+1}} (t_n - s)^{-\alpha} \left[\frac{v(x,t_{k+1}) - v(x,t_k)}{\Delta t_{k+1}} \right] ds + R^n, \\
&= \frac{1}{\Gamma(2-\alpha)} \sum_{k=0}^{n-1} \left[\frac{v(x,t_{k+1}) - v(x,t_k)}{\Delta t_{k+1}} \right] \left[(t_n - t_k)^{1-\alpha} - (t_n - t_{k+1})^{1-\alpha} \right] + R^n, \\
&= \frac{1}{\Gamma(2-\alpha)} \sum_{k=1}^{n-1} (w_{n,k+1} - w_{n,k})\, v(x,t_{n-k}) + \frac{w_{n,1}}{\Gamma(2-\alpha)} v(x,t_n) - \frac{w_{n,n}}{\Gamma(2-\alpha)} \\
&\qquad \times v(x,t_0) + R^n, \qquad (4.5)
\end{aligned}$$

where R^n denotes the truncation error term, and the coefficients $w_{n,k}$ are given by

$$w_{n,k} = \frac{(t_n - t_{n-k})^{1-\alpha} - (t_n - t_{n-k+1})^{1-\alpha}}{\Delta t_{n-k+1}}. \qquad (4.6)$$

Lemma 4.1. *The coefficients $w_{n,k}$ satisfy [103]*

(a). $w_{n,1} = \Delta t_n^{-\alpha}$.

(b). $w_{n,k} > 0, \quad 1 \leq k \leq n-1.$

(c). $w_{n,k+1} \leq w_{n,k}, \quad 1 \leq k \leq n-1.$

(d). $\sum_{k=1}^{n-1} (w_{n,k} - w_{n,k+1}) + w_{n,n} = w_{n,1}.$

(e). $(1-\alpha)(t_n - t_{n-k})^{-\alpha} \leq w_{n,k} \leq (1-\alpha)(t_n - t_{n-k+1})^{-\alpha}, \quad 1 \leq k \leq n-1.$

Lemma 4.2. *The bound of the truncation error term R^n is given in two cases as follows:*

(a). For sufficiently smooth solution $v(x,t)$ of (4.1)-(4.2) on uniform time spacing with mesh width Δt, there exists a constant c such that

$$|R^n| \leq c\Delta t^{2-\alpha}, \quad \forall t_n \in (0,T]. \tag{4.7}$$

(b). For non-smooth solution $v(x,t)$ of (4.1)-(4.2) satisfying Theorem 4.1 on non-uniform graded time spacing defined in (4.4), there exists a constant c such that

$$|R^n| \leq cn^{-\min\{2-\alpha,\theta\alpha\}}, \quad \forall t_n \in (0,T]. \tag{4.8}$$

Proof. See [60] for the proof of (a) and [103, Lemma 5.2] for the proof of (b). □

Now consider problem (4.1) at time level t_n, $1 \leq n \leq N_t$. Using the time discretization of Caputo derivative given in (4.5), we have

$$\sum_{k=1}^{n-1} \frac{(w_{n,k+1} - w_{n,k})}{\Gamma(2-\alpha)} v(x,t_{n-k}) + \frac{w_{n,1}}{\Gamma(2-\alpha)} v(x,t_n) - \frac{w_{n,n}}{\Gamma(2-\alpha)} v(x,t_0) - \mu_d \frac{\partial^2 v(x,t_n)}{\partial x^2}$$
$$+ q(t_n)v(x,t_n) + R^n = F(x,t_n), \; 1 \leq n \leq N_t, \tag{4.9}$$

$$\begin{aligned} v(x,t_0) &= g(x), \quad x \in [0,b], \\ v(0,t_n) &= 0, \qquad 1 \leq n \leq N_t, \\ v(b,t_n) &= 0, \qquad 1 \leq n \leq N_t. \end{aligned} \tag{4.10}$$

4.2.2 The spatial discretization

In this section, we introduce a cubic spline approximation method [81–83, 90] for the spatial discretization of (4.9)-(4.10). Let N_x be an positive integer. We divide the interval $[0,b]$ into N_x subintervals with $0 = x_0 < x_1 < \cdots < x_{N_x} = b$ and $x_m = mh$, $0 \leq m \leq N_x$, and $h = \frac{b}{N_x}$. Let ${}_mS_n(x)$ be the cubic spline interpolate defined on each subintervals $[x_m, x_{m+1}]$ for all $0 \le m \le N_x - 1$ and at the time level t_n, for the given values $(V_m^n)_{m=0}^{N_x}$ of the function $v(x, t_n)$ at the nodal points $x_0, x_1, \dots, x_{N_x}$. We have

$$
\begin{aligned}
{}_mS_n(x) = {} & M_m^n \frac{(x_{m+1} - x)^3}{6h} + M_{m+1}^n \frac{(x - x_m)^3}{6h} + \left(V_m^n - \frac{h^2}{6} M_m^n \right) \frac{(x_{m+1} - x)}{h} \\
& + \left(V_{m+1}^n - \frac{h^2}{6} M_{m+1}^n \right) \frac{(x - x_m)}{h}, \quad \forall\, x \in [x_m, x_{m+1}], \;\; 0 \le m \le N_x - 1,
\end{aligned}
\tag{4.11}
$$

where $M_m^n = {}_mS_n''(x_m)$, $0 \le m \le N_x - 1$. The following cubic spline identity relation can be obtained using the above equation:

$$
\frac{V_{m+1}^n - 2V_m^n + V_{m-1}^n}{h^2} = \frac{1}{6} M_{m-1}^n + \frac{4}{6} M_m^n + \frac{1}{6} M_{m+1}^n, \quad 1 \le m \le N_x - 1, \tag{4.12}
$$

which ensures the continuity of ${}_mS_n'(x)$ at the interior nodes.

The semi-discrete problem (4.9) at $x = x_m$ can be written in the following form

$$
\begin{aligned}
\frac{\partial^2 v(x_m, t_n)}{\partial x^2} = \frac{1}{\mu_d} \Bigg[& \frac{w_{n,1}}{\Gamma(2-\alpha)} v(x_m, t_n) - \frac{w_{n,n}}{\Gamma(2-\alpha)} v(x_m, t_0) + \sum_{k=1}^{n-1} \frac{(w_{n,k+1} - w_{n,k})}{\Gamma(2-\alpha)} \\
& \times v(x_m, t_{n-k}) + q(t_n) v(x_m, t_n) - F(x_m, t_n) + R^n \Bigg].
\end{aligned}
\tag{4.13}
$$

Since the exact solution $v(x, t)$ of problem (4.1) at $t = t_n$ is approximated by the cubic spline ${}_mS_n(x)$, it follows that ${}_mS_n''(x_m) = M_m^n$ is an approximation to $\frac{\partial^2 v(x_m, t_n)}{\partial x^2}$. Hence, from equation (4.13) we set

$$
\begin{aligned}
M_m^n = \frac{1}{\mu_d} \Bigg[& \frac{w_{n,1}}{\Gamma(2-\alpha)} V_m^n - \frac{w_{n,n}}{\Gamma(2-\alpha)} V_m^0 + \sum_{k=1}^{n-1} \frac{(w_{n,k+1} - w_{n,k})}{\Gamma(2-\alpha)} V_m^{n-k} + q(t_n) V_m^n \\
& - F(x_m, t_n) \Bigg].
\end{aligned}
\tag{4.14}
$$

Thus, we have

$$M_m^n = \frac{\partial^2 v(x_m, t_n)}{\partial x^2} + R^n. \tag{4.15}$$

Now substitution of equation (4.14) in equation (4.12) yields the following cubic spline approximation method for the solution $v(x, t_n)$ at x_m's :

$$\frac{w_{n,1}}{\Gamma(2-\alpha)} H_c V_m^n - \frac{w_{n,n}}{\Gamma(2-\alpha)} H_c V_m^0 + \frac{1}{\Gamma(2-\alpha)} \sum_{k=1}^{n-1} (w_{n,k+1} - w_{n,k}) H_c V_m^{n-k} - \mu_d \delta_x^2 V_m^n$$
$$+ q(t_n) H_c V_m^n = H_c F_m^n, \quad 1 \le m \le N_x - 1, 1 \le n \le N_t, \tag{4.16}$$

$$\begin{aligned} &V_m^0 = g(x_m), \quad 0 \le m \le N_x, \\ &V_0^n = 0, \quad 1 \le n \le N_t, \\ &V_{N_x}^n = 0, \quad 1 \le n \le N_t, \end{aligned} \tag{4.17}$$

where

$$H_c V_m^n = \begin{cases} \frac{1}{6} V_{m-1}^n + \frac{4}{6} V_m^n + \frac{1}{6} V_{m+1}^n, & 1 \le m \le N_x - 1, \\ V_m^n, & m = 0 \text{ or } N_x, \end{cases} \tag{4.18}$$

and

$$\delta_x^2 V_m^n = \frac{V_{m+1}^n - 2V_m^n + V_{m-1}^n}{h^2}. \tag{4.19}$$

Note that

$$H_c V_m^n = \left(I + \frac{h^2}{6} \delta_x^2 \right) V_m^n, \quad 1 \le m \le N_x - 1. \tag{4.20}$$

Lemma 4.3. *Let $\hat{T}_m^n$ be the local truncation error of the numerical scheme (4.16)-(4.17). Then*

$$\hat{T}_m^n = \begin{cases} \mathcal{O}(h^2, \Delta t^{2-\alpha}), & \text{for smooth solution on uniform time spacing,} \\ \mathcal{O}(h^2, n^{-\min\{2-\alpha, \theta\alpha\}}), & \text{for non-smooth solution on non-uniform graded} \\ & \text{time spacing.} \end{cases} \tag{4.21}$$

Proof. Note that equation (4.12) is equivalent to equation (4.16). So, the local truncation error of equation (4.12) is given as

$$\hat{T}_m^n = \frac{1}{h^2}[v(x_{m+1}, t_n) - 2v(x_m, t_n) + v(x_{m-1}, t_n)] - H_c M_m^n, \tag{4.22}$$

which on using equation (4.15) yields

$$\hat{T}_m^n = \frac{1}{h^2}[v(x_{m+1}, t_n) - 2v(x_m, t_n) + v(x_{m-1}, t_n)] - H_c \frac{\partial^2 v(x_m, t_n)}{\partial x^2} + R^n.$$

Now using Taylor expansions, we have the proof. □

4.3 Stability and convergence analysis

In this section we provide the stability and convergence analysis for both smooth and non-smooth solutions.

4.3.1 Stability and convergence analysis for smooth solution

First, we introduce some notation and prove a few lemmas that will be useful for stability and convergence analysis for the smooth solution.

Let $\mathcal{D}_h = \{u | (u_0, u_1, \cdots, u_{N_x}), u_0 = u_{N_x} = 0\}$. Then, for any u, $\vartheta \in \mathcal{D}_h$, we define the discrete inner product, $\mathcal{L}_2$ norm, H^1 semi-norm, and $\mathcal{L}_\infty$ norm as follows:

$$\langle u, \vartheta \rangle_h = h \sum_{m=1}^{N_x - 1} u_m \cdot \vartheta_m, \qquad \|u\|_h = \sqrt{\langle u, u \rangle_h},$$
$$\|\delta_x u\|_h = \sqrt{h \sum_{m=1}^{N_x} \left(\delta_x u_{m-\frac{1}{2}}\right)^2}, \quad \|u\|_\infty = \max_{1 \le m \le N_x - 1} |u_m|,$$

$$\text{where } \delta_x u_{m-\frac{1}{2}} = \frac{(u_m - u_{m-1})}{h}. \tag{4.23}$$

Similarly, we can define $\|\delta_x^2 u\|_h$ and $\|H_c u\|_h$. Now we define the inner product $\langle , \rangle_S$ for any grid functions u, $\vartheta \in \mathcal{D}_h$ as follows

$$\langle u, \vartheta \rangle_S = h \sum_{m=1}^{N_x} \delta_x u_{m-\frac{1}{2}} \cdot \delta_x \vartheta_{m-\frac{1}{2}} - \frac{h^2}{6} h \sum_{m=1}^{N_x - 1} \delta_x^2 u_m \cdot \delta_x^2 \vartheta_m, \tag{4.24}$$

and the corresponding norm is defined by

$$\|u\|_S = \sqrt{\langle u, u \rangle_S}. \tag{4.25}$$

Lemma 4.4. *For any grid function $u \in \mathcal{D}_h$, the following inequality holds*

$$\|u\|_\infty \le \frac{\sqrt{b}}{2} \|\delta_x u\|_h.$$

Proof. See [95] for the proof. □

Lemma 4.5. *For any grid function $u \in \mathcal{D}_h$, the following inequality holds*

$$\frac{1}{3} \|\delta_x u\|_h^2 \le \|u\|_S^2 \le \|\delta_x u\|_h^2.$$

Proof. From equation (4.24) we have

$$\begin{aligned} \|u\|_S^2 &= h \sum_{m=1}^{N_x} \left(\delta_x u_{m-\frac{1}{2}} \right)^2 - \frac{h^2}{6} h \sum_{m=1}^{N_x - 1} \left(\delta_x^2 u_m \right)^2, \\ &\le h \sum_{m=1}^{N_x} \left(\delta_x u_{m-\frac{1}{2}} \right)^2, \\ &= \|\delta_x u\|_h^2. \end{aligned}$$

Now

$$
\begin{aligned}
\|u\|_S^2 &= h\sum_{m=1}^{N_x}\left(\delta_x u_{m-\frac{1}{2}}\right)^2 - \frac{h^2}{6}h\sum_{m=1}^{N_x-1}\left(\delta_x^2 u_m\right)^2, \\
&= \|\delta_x u\|_h^2 - \frac{h^2}{6}\|\delta_x^2 u\|_h^2, \\
&\geq \frac{1}{3}\|\delta_x u\|_h^2, \quad \left(\text{using the inverse estimate} \|\delta_x^2 u\|_h \leq \frac{2}{h}\|\delta_x u\|_h\right).
\end{aligned}
$$

Thus, we have the proof. □

Lemma 4.6. *For any grid functions $u, \vartheta \in \mathcal{D}_h$, the following result holds*

$$
\langle u, \vartheta\rangle_S = -h\sum_{m=1}^{N_x-1}(H_c u_m)\cdot(\delta_x^2\vartheta_m).
$$

Proof. We proceed as follows

$$
\begin{aligned}
-h\sum_{m=1}^{N_x-1}(H_c u_m)\cdot(\delta_x^2\vartheta_m) &= -h\sum_{m=1}^{N_x-1}\left(I+\frac{h^2}{6}\delta_x^2\right)u_m\cdot\delta_x^2\vartheta_m, \\
&= -h\sum_{m=1}^{N_x-1}u_m\cdot\delta_x^2\vartheta_m - \frac{h^2}{6}h\sum_{m=1}^{N_x-1}\delta_x^2 u_m\cdot\delta_x^2\vartheta_m,
\end{aligned}
$$

Using the discrete Green's formula and $u_0 = u_{N_x} = \vartheta_0 = \vartheta_{N_x} = 0$, we get

$$
\begin{aligned}
-h\sum_{m=1}^{N_x-1}(H_c u_m)\cdot(\delta_x^2\vartheta_m) &= h\sum_{m=1}^{N_x}\delta_x u_{m-\frac{1}{2}}\cdot\delta_x\vartheta_{m-\frac{1}{2}} - \frac{h^2}{6}h\sum_{m=1}^{N_x-1}\delta_x^2 u_m\cdot\delta_x^2\vartheta_m, \\
&= \langle u, \vartheta\rangle_S.
\end{aligned}
$$

□

Theorem 4.2. *The solution of the discrete problem (4.16)-(4.17) on uniform mesh satisfies*

$$
\|V^n\|_S^2 \leq \|V^0\|_S^2 + c\max_{1\leq l\leq N_t}\|H_c F^l\|_h^2. \tag{4.26}
$$

Proof. It follows from equation (4.16) that

$$\frac{w_{n,1}}{\Gamma(2-\alpha)} H_c V_m^n - \frac{w_{n,n}}{\Gamma(2-\alpha)} H_c V_m^0 + \frac{1}{\Gamma(2-\alpha)} \sum_{k=1}^{n-1} \left(w_{n,k+1} - w_{n,k}\right) H_c V_m^{n-k} - \mu_d \delta_x^2 V_m^n + q(t_n) H_c V_m^n = H_c F_m^n.$$

Multiplying the above equation by $-2h\delta_x^2 V_m^n$, summing over m for $m = 1, 2, \ldots, N_x - 1$, and using Lemma 4.5, we have

$$\frac{2w_{n,1}}{\Gamma(2-\alpha)} \|V^n\|_S^2 - \frac{2w_{n,n}}{\Gamma(2-\alpha)} \langle V^0, V^n \rangle_S = \frac{2}{\Gamma(2-\alpha)} \sum_{k=1}^{n-1} \left(w_{n,k} - w_{n,k+1}\right) \langle V^{n-k}, V^n \rangle_S \\ -2\mu_d \|\delta_x^2 V^n\|_h^2 - 2q(t_n) \|V^n\|_S^2 - 2\langle H_c F^n, \delta_x^2 V^n \rangle_h,$$

which gives

$$\left(\frac{2w_{n,1}}{\Gamma(2-\alpha)} + 2q(t_n) \right) \|V^n\|_S^2 + 2\mu_d \|\delta_x^2 V^n\|_h^2 = \frac{2}{\Gamma(2-\alpha)} \sum_{k=1}^{n-1} \left(w_{n,k} - w_{n,k+1}\right) \langle V^{n-k}, V^n \rangle_S \\ + \frac{2w_{n,n}}{\Gamma(2-\alpha)} \langle V^0, V^n \rangle_S - 2\langle H_c F^n, \delta_x^2 V^n \rangle_h.$$

Thus

$$\frac{2w_{n,1}}{\Gamma(2-\alpha)} \|V^n\|_S^2 + 2\mu_d \|\delta_x^2 V^n\|_h^2 \leq \frac{1}{\Gamma(2-\alpha)} \sum_{k=1}^{n-1} \left(w_{n,k} - w_{n,k+1}\right) \left(\|V^{n-k}\|_S^2 \right. \\ \left. + \|V^n\|_S^2 \right) + \frac{w_{n,n}}{\Gamma(2-\alpha)} (\|V^0\|_S^2 + \|V^n\|_S^2) + 2\mu_d \|\delta_x^2 V^n\|_h^2 + \frac{1}{2\mu_d} \|H_c F^n\|_h^2.$$

Hence,

$$\frac{2w_{n,1}}{\Gamma(2-\alpha)} \|V^n\|_S^2 \;\leq\; \frac{1}{\Gamma(2-\alpha)} \sum_{k=1}^{n-1} (w_{n,k} - w_{n,k+1}) \|V^{n-k}\|_S^2 + \frac{w_{n,1}}{\Gamma(2-\alpha)} \|V^n\|_S^2 + \\ \frac{w_{n,n}}{\Gamma(2-\alpha)} \|V^0\|_S^2 + \frac{1}{2\mu_d} \|H_c F^n\|_h^2,$$

which is equivalent to

$$w_{n,1}\|V^n\|_S^2 \leq \sum_{k=1}^{n-1}(w_{n,k}-w_{n,k+1})\|V^{n-k}\|_S^2 + w_{n,n}\|V^0\|_S^2 + \frac{\Gamma(2-\alpha)}{2\mu_d}\|H_cF^n\|_h^2.$$

Equivalently,

$$w_{n,1}\|V^n\|_S^2 \leq \sum_{k=1}^{n-1}(w_{n,k}-w_{n,k+1})\|V^{n-k}\|_S^2 + w_{n,n}\left[\|V^0\|_S^2 + \frac{\Gamma(2-\alpha)}{2\mu_d w_{n,n}}\|H_cF^n\|_h^2\right].$$

Noticing that $w_{n,n} > \dfrac{T^{-\alpha}}{\Gamma(1-\alpha)}$, we have

$$\begin{aligned} w_{n,1}\|V^n\|_S^2 \leq& \sum_{k=1}^{n-1}(w_{n,k}-w_{n,k+1})\|V^{n-k}\|_S^2 \\ &+ w_{n,n}\left[\|V^0\|_S^2 + \frac{T^{\alpha}(1-\alpha)(\Gamma(1-\alpha))^2}{2\mu_d}\|H_cF^n\|_h^2\right]. \end{aligned} \tag{4.27}$$

We denote

$$\chi = \|V^0\|_S^2 + \frac{T^{\alpha}(1-\alpha)(\Gamma(1-\alpha))^2}{2\mu_d}\max_{1\leq l\leq N_t}\|H_cF^l\|_h^2.$$

Hence, from equation (4.27), we get

$$w_{n,1}\|V^n\|_S^2 \leq \sum_{k=1}^{n-1}(w_{n,k}-w_{n,k+1})\|V^{n-k}\|_S^2 + w_{n,n}\chi. \tag{4.28}$$

Now we prove by induction that

$$\|V^n\|_S^2 \leq \chi, \quad 1\leq n\leq N_t. \tag{4.29}$$

Put $n=1$ in equation (4.28) to get

$$\|V^1\|_S^2 \leq \chi,$$

which is identical to (4.29) for $n = 1$. Now let us assume that (4.29) holds for $n = 1, 2, \ldots, j-1$, that is

$$\|V^n\|_S^2 \leq \chi, \quad 1 \leq n \leq j-1. \tag{4.30}$$

The inequality (4.28) together with assumption (4.30) yield

$$\begin{aligned} w_{j,1}\|V^j\|_S^2 &\leq \sum_{k=1}^{j-1}(w_{j,k} - w_{j,k+1})\,\|V^{j-k}\|_S^2 + w_{j,j}\chi, \\ &\leq \left[\sum_{k=1}^{j-1}(w_{j,k} - w_{j,k+1}) + w_{j,j}\right]\chi = w_{j,1}\chi. \end{aligned}$$

Thus, (4.29) holds for all n. Hence, we have the proof. □

Now we will prove the main convergence theorem.

Theorem 4.3. *Let $v(x,t)$ be the sufficiently smooth solution of problem (4.1)-(4.2) and let $\{V_m^n, 0 \leq m \leq N_x, 1 \leq n \leq N_t\}$ be the solution of the discrete problem (4.16)-(4.17) on uniform mesh. Then, the following result holds*

$$\|v(.,t_n) - V^n\|_\infty \leq c(h^2 + \Delta t^{2-\alpha}).$$

Proof. Recall that the exact solution of the considered problem (4.1)-(4.2) is $v(x_m, t_n)$ at $x = x_m$ and $t = t_n$ and V_m^n is the approximate value of $v(x_m, t_n)$. Now we define $e_m^n = v(x_m, t_n) - V_m^n$ for $0 \leq m \leq N_x$, and $1 \leq n \leq N_t$. Since $v(x_m, t_n)$ is the exact solution, from (4.16) we have

$$\begin{aligned} &\frac{w_{n,1}}{\Gamma(2-\alpha)}H_c v(x_m, t_n) - \frac{w_{n,n}}{\Gamma(2-\alpha)}H_c v(x_m, t_0) + \frac{1}{\Gamma(2-\alpha)}\sum_{k=1}^{n-1}(w_{n,k+1} - w_{n,k}) \\ &\quad \times H_c v(x_m, t_{n-k}) - \mu_d \delta_x^2 v(x_m, t_n) + q(t_n) H_c v(x_m, t_n) = H_c F_m^n + \hat{T}_m^n, \\ &\qquad\qquad 1 \leq m \leq N_x - 1, 1 \leq n \leq N_t. \end{aligned} \tag{4.31}$$

Using (4.16)-(4.17), it is evident that the error equation is given by

$$\frac{w_{n,1}}{\Gamma(2-\alpha)} H_c e_m^n + \frac{1}{\Gamma(2-\alpha)} \sum_{k=1}^{n-1} \left(w_{n,k+1} - w_{n,k}\right) H_c e_m^{n-k} - \mu_d \delta_x^2 e_m^n + q(t_n) H_c e_m^n = \hat{T}_m^n,$$
$$1 \leq m \leq N_x - 1, \; 1 \leq n \leq N_t, \tag{4.32}$$

$$\begin{aligned} e_m^0 &= 0, \quad 0 \leq m \leq N_x, \\ e_0^n &= 0, \quad 1 \leq n \leq N_t, \\ e_{N_x}^n &= 0, \quad 1 \leq n \leq N_t. \end{aligned} \tag{4.33}$$

Now applying Theorem 4.2 for the error equation (4.32)-(4.33) we have

$$\|e^n\|_S^2 \leq c \max_{1 \leq l \leq N_t} \|\hat{T}^l\|_h^2, \quad 1 \leq n \leq N_t.$$

Now for the smooth solution on the uniform mesh, Lemma 4.3 implies that

$$\max_{1 \leq l \leq N_t} \|\hat{T}^l\|_h \leq c(h^2 + \Delta t^{2-\alpha}),$$

$$\|e^n\|_S^2 \leq c(h^2 + \Delta t^{2-\alpha})^2. \tag{4.34}$$

Thus, using Lemmas 4.4 and 4.5 with equation (4.34), we have

$$\|e^n\|_\infty^2 \leq \frac{b}{4} \|\delta_x u\|_h^2 \leq \frac{3b}{4} \|e^n\|_S^2 \leq c(h^2 + \Delta t^{2-\alpha})^2,$$

Hence,

$$\|v(.,t_n) - V^n\|_\infty \leq c(h^2 + \Delta t^{2-\alpha}).$$

Thus, we have the proof. □

4.3.2 Stability and convergence analysis for non-smooth solution

Now we provide the stability and convergence analysis of the numerical scheme (4.16)-(4.17) on a non-uniform graded mesh for the non-smooth solution. Owing to the presence of the cubic spline difference operator, we were unable to pursue the analysis on a graded mesh as recommended in [103]. Instead, we employed the Fourier analysis method to investigate stability and convergence of the discrete problem (4.16)-(4.17) on the non-uniform graded mesh.

Let the scheme (4.16)-(4.17) having a perturbed solution $\{\widetilde{V}_m^n, 1 \leq m \leq N_x - 1,\ 1 \leq n \leq N_t\}$. Then, we will examine how the perturbation $\zeta_m^n = V_m^n - \widetilde{V}_m^n,\ 1 \leq m \leq N_x - 1,\ 1 \leq n \leq N_t$, evolves over time. Note that ζ_m^n satisfies the following error equation

$$\begin{aligned}\frac{w_{n,1}}{\Gamma(2-\alpha)} H_c\zeta_m^n - \frac{w_{n,n}}{\Gamma(2-\alpha)} H_c\zeta_m^0 + \frac{1}{\Gamma(2-\alpha)} \sum_{k=1}^{n-1} \left(w_{n,k+1} - w_{n,k}\right) H_c\zeta_m^{n-k} - \mu_d \delta_x^2 \zeta_m^n \\ + q(t_n) H_c\zeta_m^n = 0, \quad 1 \leq m \leq N_x - 1, 1 \leq n \leq N_t, \end{aligned} \tag{4.35}$$

$$\begin{aligned} &\zeta_m^0 = g(x_m) - \bar{g}(x_m),\ 0 \leq m \leq N_x, \\ &\zeta_0^n = 0, \quad 1 \leq n \leq N_t, \\ &\zeta_{N_x}^n = 0, \quad 1 \leq n \leq N_t, \end{aligned} \tag{4.36}$$

where $\bar{g}(x_m) = \widetilde{V}_m^0$. Further, utilizing the Definition 4.18, we could easily obtain the following scheme

$$\begin{aligned} A_1^*\zeta_{m+1}^n + A_2^*\zeta_m^n + A_1^*\zeta_{m-1}^n = \frac{w_{n,n}}{\Gamma(2-\alpha)} H_c\zeta_m^0 + \frac{1}{\Gamma(2-\alpha)} \sum_{k=1}^{n-1} \left(w_{n,k} - w_{n,k+1}\right) \\ \times H_c\zeta_m^{n-k},\ 1 \leq m \leq N_x, \end{aligned} \tag{4.37}$$

where

$$A_1^* = \frac{1}{6}\left[\frac{w_{n,1}}{\Gamma(2-\alpha)} + q(t_n)\right] - \frac{\mu_d}{h^2}, \quad A_2^* = \frac{4}{6}\left[\frac{w_{n,1}}{\Gamma(2-\alpha)} + q(t_n)\right] + \frac{2\mu_d}{h^2}. \tag{4.38}$$

For $0 \leq n \leq N_t$, we define the following grid function

$$\zeta^n(x) = \begin{cases} \zeta_m^n, & \text{if } x \in \left(x_{m-\frac{1}{2}}, x_{m+\frac{1}{2}}\right], \ 1 \leq m \leq N_x - 1, \\ 0, & \text{if } x \in \left[0, \frac{h}{2}\right] \cup \left(x_{N_x} - \frac{h}{2}, x_{N_x}\right]. \end{cases}$$

The Fourier series expansion of the grid function $\zeta^n(x)$ is defined by

$$\zeta^n(x) = \sum_{k=-\infty}^{\infty} \xi^n(k) e^{-\frac{2\pi k x}{x_{N_x}}}, \tag{4.39}$$

where $\xi^n(k)$ is the Fourier coefficient of $\zeta^n(x)$ and is given by

$$\xi^n(k) = \frac{1}{x_{N_x}} \int_0^{x_{N_x}} \zeta^n(x) e^{-\frac{2\pi k x}{x_{N_x}}} dx.$$

To facilitate our analysis, we define the following norm

$$\|\zeta^n\|_h = \left(\sum_{m=1}^{N_x-1} h|\zeta_m^n|^2\right)^{1/2}, \quad 0 \leq n \leq N_t.$$

With the help of Parseval identity, we obtain

$$\|\zeta^n\|_h = \left[x_{N_x} \sum_{k=-\infty}^{\infty} |\xi^n(k)|^2\right]^{1/2}, \quad 0 \leq n \leq N_t. \tag{4.40}$$

We assume the solution of the equation (4.35)-(4.36) takes the following form

$$\zeta_m^n = \xi^n e^{i\rho m h}, \tag{4.41}$$

where $i = \sqrt{-1},\ \rho = \frac{2\pi k}{b}$. Substituting (4.41) in (4.37), we could easily obtain

$$\xi^n \left(A_1^* e^{i\rho h} + A_2^* + A_1^* e^{-i\rho h}\right) = \frac{1}{\Gamma(2-\alpha)} \left[\sum_{k=1}^{n-1} (w_{n,k} - w_{n,k+1})\xi^{n-k} + w_{n,n}\xi^0\right] \times \left(\frac{1}{6}e^{i\rho h} + \frac{4}{6} + \frac{1}{6}e^{-i\rho h}\right),\ 1 \le n \le N_t.$$

Using Euler's formula, we simply obtain

$$\xi^n \left(2A_1^* \cos(\rho h) + A_2^*\right) = \frac{1}{6}\left(2\cos(\rho h) + 4\right) \left[\frac{1}{\Gamma(2-\alpha)} \sum_{k=1}^{n-1} (w_{n,k} - w_{n,k+1})\xi^{n-k} + \frac{w_{n,n}}{\Gamma(2-\alpha)}\xi^0\right],\ 1 \le n \le N_t.$$

The above equations can be simplified to

$$\xi^n = \frac{\left[\frac{w_{n,n}}{\Gamma(2-\alpha)}\xi^0 + \frac{1}{\Gamma(2-\alpha)} \sum_{k=1}^{n-1} (w_{n,k} - w_{n,k+1})\xi^{n-k}\right]}{\left[\frac{w_{n,1}}{\Gamma(2-\alpha)} + q(t_n) + \frac{12\mu_d}{h^2} \frac{(1-\cos(\rho h))}{(2\cos(\rho h)+4)}\right]},\quad 1 \le n \le N_t. \tag{4.42}$$

In the following lemma, we analyze the solution ξ^n in order to establish the stability of the numerical scheme (4.16)-(4.17).

Lemma 4.7. *Consider ξ^n to be the solution of equation (4.42). Then,*

$$|\xi^n| \le |\xi^0|,\ 1 \le n \le N_t.$$

Proof. We shall establish the validity of this statement by employing the principle of mathematical induction. By substituting $n = 1$ into equation (4.42), we obtain

$$|\xi^1| = \left| \frac{\frac{w_{1,1}}{\Gamma(2-\alpha)}\xi^0}{\frac{w_{1,1}}{\Gamma(2-\alpha)} + q(t_1) + \frac{12\mu_d}{h^2} \frac{(1-\cos(\rho h))}{(2\cos(\rho h)+4)}} \right| \le |\xi^0|,$$

since, $q \geq 0$ and $\mu_d > 0$. Now, let us assume that

$$|\xi^l| \leq |\xi^0|, \text{ for all } 1 \leq l \leq n-1. \tag{4.43}$$

Next, for $l = n$, from equation (4.42) with Lemma 4.1 and assumptions (4.43), we get

$$|\xi^n| \leq \frac{\left|\frac{w_{n,n}}{\Gamma(2-\alpha)} + \frac{1}{\Gamma(2-\alpha)}\sum_{k=1}^{n-1}(w_{n,k} - w_{n,k+1})\right||\xi^0|}{\left|\frac{w_{n,1}}{\Gamma(2-\alpha)} + q(t_n) + \frac{12\mu_d}{h^2}\frac{(1-\cos(\rho h))}{(2\cos(\rho h)+4)}\right|} \leq |\xi^0|,$$

Thus, we have $|\xi^n| \leq |\xi^0|$, for all $1 \leq n \leq N_t$. □

Theorem 4.4. *The cubic spline difference scheme given by (4.16)-(4.17) on a non--uniform graded mesh for the non-smooth solution, for solving the model problem (4.1)-(4.2) is unconditionally stable.*

Proof. By considering equation (4.40) and Lemma 4.7 together, one can obtain the following inequality

$$\|\zeta^n\|_h = \left[x_{N_x}\sum_{k=-\infty}^{\infty}|\xi^n(k)|^2\right]^{\frac{1}{2}} \leq \left[x_{N_x}\sum_{k=-\infty}^{\infty}|\xi^0(k)|^2\right]^{\frac{1}{2}} = \|\zeta^0\|_h, \quad 1 \leq n \leq N_t. \tag{4.44}$$

Thus, $\|\zeta^n\|_h \leq \|\zeta^0\|_h$, $1 \leq n \leq N_t$. Hence, the numerical scheme given by (4.16)-(4.17) is unconditionally stable. □

Recall that the exact solution of the considered problem (4.1)-(4.2) is $v(x_m, t_n)$ at $x = x_m$ and $t = t_n$ and V_m^n is the approximate value of $v(x_m, t_n)$. Now we define $\varepsilon_m^n = v(x_m, t_n) - V_m^n$ for $0 \leq m \leq N_x$, and $1 \leq n \leq N_t$. Since $v(x_m, t_n)$ is the exact solution, from (4.16) we have

$$\frac{w_{n,1}}{\Gamma(2-\alpha)}H_c v(x_m, t_n) - \frac{w_{n,n}}{\Gamma(2-\alpha)}H_c v(x_m, t_0) + \frac{1}{\Gamma(2-\alpha)}\sum_{k=1}^{n-1}(w_{n,k+1} - w_{n,k})$$

$$\times H_c v(x_m, t_{n-k}) - \mu_d \delta_x^2 v(x_m, t_n) + q(t_n) H_c v(x_m, t_n) = H_c F_m^n + \hat{T}_m^n,$$
$$1 \le m \le N_x - 1, 1 \le n \le N_t. \quad (4.45)$$

Using (4.16)-(4.17), it is evident that the error equation is given by

$$\frac{w_{n,1}}{\Gamma(2-\alpha)} H_c \varepsilon_m^n + \frac{1}{\Gamma(2-\alpha)} \sum_{k=1}^{n-1} (w_{n,k+1} - w_{n,k}) H_c \varepsilon_m^{n-k} - \mu_d \delta_x^2 \varepsilon_m^n + q(t_n) H_c \varepsilon_m^n = \hat{T}_m^n,$$
$$1 \le m \le N_x - 1, 1 \le n \le N_t, \quad (4.46)$$

$$\begin{aligned} &\varepsilon_m^0 = 0, \ 0 \le m \le N_x, \\ &\varepsilon_0^n = 0, \ 1 \le n \le N_t, \\ &\varepsilon_{N_x}^n = 0, \ 1 \le n \le N_t. \end{aligned} \quad (4.47)$$

Equation 4.46 can be restated as

$$\left[\frac{1}{\Gamma(2-\alpha)} + q(t_n) \frac{1}{w_{n,1}}\right] H_c \varepsilon_m^n + \frac{1}{\Gamma(2-\alpha)} \sum_{k=1}^{n-1} \frac{(w_{n,n-k+1} - w_{n,n-k})}{w_{n,1}} H_c \varepsilon_m^k$$
$$= \frac{\mu_d}{w_{n,1}} \delta_x^2 \varepsilon_m^n + \mathfrak{T}_m^n, \ 1 \le m \le N_x - 1, 1 \le n \le N_t, \quad (4.48)$$

where $\mathfrak{T}_m^n = \frac{\hat{T}_m^n}{w_{n,1}}$. Now combining Lemma 4.1, Lemma 4.3, and a result from [103, Eq. (5.1), p.1069], we arrive at

$$\begin{aligned} |\mathfrak{T}_m^n| = \left|\frac{\hat{T}_m^n}{w_{n,1}}\right| &\le \frac{c(h^2 + n^{-\min\{2-\alpha,\theta\alpha\}})}{w_{n,1}} = \frac{c\left(h^2 + n^{-\min\{2-\alpha,\theta\alpha\}}\right)}{\Delta t_n^{-\alpha}} \\ &\le c\left(h^2 + \Delta t_n^{\alpha} n^{-\min\{2-\alpha,\theta\alpha\}}\right) \\ &\le c\left(h^2 + (CT)^{\alpha} \left(\frac{n}{N_t}\right)^{\theta\alpha} n^{-\min\{2-\alpha,\theta\alpha\}}\right) \\ &\le c\left(h^2 + (CT)^{\alpha} \left(\frac{n}{N_t}\right)^{\min\{2-\alpha,\theta\alpha\}} n^{-\min\{2-\alpha,\theta\alpha\}}\right), \end{aligned}$$

since $\frac{n}{N_t} \leq 1$ and C is a generic constant independent of time and space step-lengths. Therefore, we write

$$|\mathcal{T}_m^n| \leq c\left(h^2 + N_t^{-\min\{2-\alpha,\theta\alpha\}}\right). \tag{4.49}$$

Moreover, in view of cubic spline operator H_c defined in (4.18) we obtain the following equivalent form of the scheme (4.48)

$$A_3^*\varepsilon_{m+1}^n + A_4^*\varepsilon_m^n + A_3^*\varepsilon_{m-1}^n = \frac{1}{\Gamma(2-\alpha)}\sum_{k=1}^{n-1}(w_{n,k} - w_{n,k+1})H_c\varepsilon_m^{n-k} + \mathcal{T}_m^n,$$
$$1 \leq m \leq N_x - 1,\ 1 \leq n \leq N_t, \tag{4.50}$$

where

$$A_3^* = \frac{1}{6}\left[\frac{1}{\Gamma(2-\alpha)} + \frac{q(t_n)}{w_{n,1}}\right] - \frac{\mu_d}{w_{n,1}h^2},\quad A_4^* = \frac{4}{6}\left[\frac{1}{\Gamma(2-\alpha)} + \frac{q(t_n)}{w_{n,1}}\right] + \frac{2\mu_d}{w_{n,1}h^2}. \tag{4.51}$$

Further, for $0 \leq n \leq N_t$, we define the following grid functions

$$\varepsilon^n(x) = \begin{cases} \varepsilon_m^n, & \text{if } x \in \left(x_{m-\frac{1}{2}}, x_{m+\frac{1}{2}}\right],\quad 1 \leq m \leq N_x - 1, \\ 0, & \text{if } x \in \left[0, \frac{h}{2}\right] \cup \left(x_{N_x} - \frac{h}{2}, x_{N_x}\right], \end{cases}$$

and

$$\mathcal{T}^n(x) = \begin{cases} \mathcal{T}_m^n, & \text{if } x \in \left(x_{m-\frac{1}{2}}, x_{m+\frac{1}{2}}\right],\quad 1 \leq m \leq N_x - 1, \\ 0, & \text{if } x \in \left[0, \frac{h}{2}\right] \cup \left(x_{N_x} - \frac{h}{2}, x_{N_x}\right]. \end{cases}$$

The Fourier series expansions of $\varepsilon^n(x)$ and $\mathcal{T}^n(x)$ are defined by

$$\varepsilon^n(x) = \sum_{k=-\infty}^{\infty}\varphi^n(k)e^{-\frac{2\pi k x}{x_{N_x}}}, \tag{4.52}$$

and

$$\mathcal{T}^n(x) = \sum_{k=-\infty}^{\infty}\upsilon^n(k)e^{-\frac{2\pi k x}{x_{N_x}}}, \tag{4.53}$$

where the respective Fourier coefficient $\varphi^n(k)$ and $\upsilon^n(k)$ are defined by

$$\varphi^n(k) = \frac{1}{x_{N_x}} \int_0^{x_{N_x}} \varepsilon^n(x) e^{-\frac{2\pi k x}{x_{N_x}}} dx,$$

and

$$\upsilon^n(k) = \frac{1}{x_{N_x}} \int_0^{x_{N_x}} \mathfrak{T}^n(x) e^{-\frac{2\pi k x}{x_{N_x}}} dx.$$

By virtue of the $\mathcal{L}_2$-discrete norm definition and Parseval's equality, we have

$$\|\varepsilon^n\|_h = \left(h \sum_{m=1}^{N_x-1} |\varepsilon_m^n|^2 \right)^{1/2} = \left[x_{N_x} \sum_{k=-\infty}^{\infty} |\varphi^n(k)|^2 \right]^{1/2}, \quad 1 \leq n \leq N_t, \tag{4.54}$$

and

$$\|\mathfrak{T}^n\|_h = \left(h \sum_{m=1}^{N_x-1} |\mathfrak{T}_m^n|^2 \right)^{1/2} = \left[x_{N_x} \sum_{k=-\infty}^{\infty} |\upsilon^n(k)|^2 \right]^{1/2}, \quad 1 \leq n \leq N_t. \tag{4.55}$$

To proceed further, we assume that

$$\varepsilon_m^n = \varphi^n e^{i\rho m h}, \quad \mathfrak{T}_m^n = \upsilon^n e^{i\rho m h}, \tag{4.56}$$

where $i = \sqrt{-1}$, $\rho = \frac{2\pi k}{b}$. Substituting (4.56) into (4.50), we could easily obtain

$$\begin{aligned} \varphi^n \left(A_3^* e^{i\rho h} + A_4^* + A_3^* e^{-i\rho h} \right) = \frac{1}{\Gamma(2-\alpha)} & \left[\sum_{k=1}^{n-1} \frac{(w_{n,k} - w_{n,k+1})}{w_{n,1}} \varphi^{n-k} \right] \\ & \times \left(\frac{1}{6} e^{i\rho h} + \frac{4}{6} + \frac{1}{6} e^{-i\rho h} \right) + \upsilon^n, \ 1 \leq n \leq N_t. \end{aligned}$$

Further, Euler's formula yields

$$\varphi^n \left(2A_3^* \cos(\rho h) + A_4^* \right) = \frac{A_5^*}{\Gamma(2-\alpha)} \sum_{k=1}^{n-1} \frac{(w_{n,k} - w_{n,k+1})}{w_{n,1}} \varphi^{n-k} + \upsilon^n,$$

where $A_5^* = \frac{(2\cos(\rho h)+4)}{6}$. The above equations can be simplified to

$$\varphi^n = \frac{\frac{A_5^*}{\Gamma(2-\alpha)}\left[\sum_{k=1}^{n-1}\frac{(w_{n,k}-w_{n,k+1})}{w_{n,1}}\varphi^{n-k}\right]+\upsilon^n}{A_5^*\left[\frac{1}{\Gamma(2-\alpha)}+\frac{q(t_n)}{w_{n,1}}\right]+\frac{2\mu_d}{w_{n,1}h^2}(1-\cos(\rho h))}. \tag{4.57}$$

The series presented in equation (4.55) converges. Hence, there exists a positive constant C_1 such that

$$|\upsilon^n| \equiv |\upsilon^n(k)| \leq C_1 \Delta t |\upsilon^1|, \tag{4.58}$$

where we set $\Delta t = \max\limits_{1\leq n\leq N_t} \Delta t_n$.

Lemma 4.8. *For $n = 1, 2, \ldots, N_t$, we have*

$$|\varphi^n| \leq 3\Gamma(2-\alpha)C_1(1+\Delta t)^n|\upsilon^1|. \tag{4.59}$$

Proof. We shall establish the validity of this statement by employing the principle of mathematical induction. By substituting $n = 1$ and using $\varphi^0 = 0$ into equation (4.57), we obtain

$$|\varphi^1| = \left|\frac{\upsilon^1}{A_5^*\left[\frac{1}{\Gamma(2-\alpha)}+\frac{q(t_1)}{w_{1,1}}\right]+\frac{2\mu_d}{w_{1,1}h^2}(1-\cos(\rho h))}\right|. \tag{4.60}$$

Moreover, for $n \geq 1$, note that

$$A_5^*\left[\frac{1}{\Gamma(2-\alpha)}+\frac{q(t_n)}{w_{n,1}}\right]+\frac{2\mu_d}{w_{n,1}h^2}(1-\cos(\rho h)) \geq \frac{A_5^*}{\Gamma(2-\alpha)} \geq \frac{1}{3\Gamma(2-\alpha)}. \tag{4.61}$$

Therefore, using (4.61) in (4.60) for $n = 1$, we get

$$|\varphi^1| \leq 3\Gamma(2-\alpha)\left|\upsilon^1\right| \leq 3\Gamma(2-\alpha)C_1(1+\Delta t)|\upsilon^1|. \tag{4.62}$$

Now, let us assume that

$$|\varphi^l| \leq 3\Gamma(2-\alpha)C_1(1+\Delta t)^l|\upsilon^1|, \text{ for all } 1 \leq l \leq n-1. \tag{4.63}$$

Next, for $l = n$, from equation (4.57) with Lemma 4.1, equation (4.58), and equation (4.61) we get

$$|\varphi^n| \leq \frac{\frac{A_5^*}{\Gamma(2-\alpha)}\left[\sum_{k=1}^{n-1}\frac{(w_{n,k}-w_{n,k+1})}{w_{n,1}}\right]\max\limits_{1\leq j\leq n-1}|\varphi^j|}{\frac{A_5^*}{\Gamma(2-\alpha)}} + \frac{|\upsilon^n|}{\frac{1}{3\Gamma(2-\alpha)}}.$$

Further, using the assumptions (4.63) with Lemma 4.1, we get

$$\begin{aligned}|\varphi^n| \leq& 3\Gamma(2-\alpha)C_1(1+\Delta t)^{n-1}|\upsilon^1| + 3\Gamma(2-\alpha)C_1(1+\Delta t)|\upsilon^1|\\ =& 3\Gamma(2-\alpha)C_1\left((1+\Delta t)^{n-1} + (1+\Delta t)\right)|\upsilon^1|.\end{aligned}$$

Ultimately, we write

$$|\varphi^n| \leq 3\Gamma(2-\alpha)C_1(1+\Delta t)^n|\upsilon^1|.$$

Thus, we have the lemma. □

Theorem 4.5. *Let $v(x,t)$ be the non-smooth solution of problem (4.1)-(4.2) and let $\{V_m^n, 0 \leq m \leq N_x, 1 \leq n \leq N_t\}$ be the solution of the discrete problem (4.16)-(4.17) on non-uniform graded mesh. Then, the following result holds*

$$\|v^n - V^n\|_h \leq c\left(h^2 + N_t^{-\min\{2-\alpha,\theta\alpha\}}\right).$$

Proof. Utilizing both equation (4.49) and the first equality of (4.55), we arrive at

$$\|\mathfrak{T}^n\|_h \leq c\sqrt{N_x h}\left(h^2 + N_t^{-\min\{2-\alpha,\theta\alpha\}}\right). \tag{4.64}$$

By invoking Lemma 4.8, along with equations (4.54), (4.55), and (4.64), for $1 \leq n \leq N_t$, we can deduce the following estimate

$$
\begin{aligned}
\|\varepsilon^n\|_h^2 =& x_{N_x} \sum_{k=-\infty}^{\infty} |\varphi^n(k)|^2 \\
\leq & x_{N_x} \sum_{k=-\infty}^{\infty} \left(3\Gamma(2-\alpha)C_1\right)^2 (1+\Delta t)^{2n} |v^1(k)|^2 \\
=& \left(3\Gamma(2-\alpha)C_1\right)^2 (1+\Delta t)^{2n} \|\mathfrak{T}^1\|_2^2 \\
\leq & \, c^2 N_x h \left(3\Gamma(2-\alpha)C_1\right)^2 (1+\Delta t)^{2n} \left(h^2 + N_t^{-\min\{2-\alpha,\theta\alpha\}}\right)^2 \\
\leq & c^2 N_x h \left(3\Gamma(2-\alpha)C_1\right)^2 \exp(2n\Delta t) \left(h^2 + N_t^{-\min\{2-\alpha,\theta\alpha\}}\right)^2.
\end{aligned}
$$

Moreover, by noting the fact that $n\Delta t \leq T$, we obtain

$$
\|\varepsilon^n\|_h \leq c \left(h^2 + N_t^{-\min\{2-\alpha,\theta\alpha\}}\right).
$$

This completes the proof. □

4.4 Numerical results

In this segment, we present results for two numerical examples to assess the practical performance of the proposed numerical scheme. If $v(x_m, t_n)$ and $V(x_m, t_n)$ are the exact and approximate solutions of problem (4.1)-(4.2) respectively at the point (x_m, t_n), then the accuracy of the numerical solution will be measured as follows

$$
\mathcal{L}_\infty(h, \Delta t) = \|v - V\|_\infty = \max_{1\leq n\leq N_t} \max_{1\leq m\leq N_x-1} |v(x_m, t_n) - V(x_m, t_n)|, \tag{4.65}
$$

$$
\mathcal{L}_2(h, \Delta t) = \|v - V\|_2 = \max_{1\leq n\leq N_t} \sqrt{h \sum_{m=1}^{N_x-1} \left(v(x_m, t_n) - V(x_m, t_n)\right)^2}. \tag{4.66}
$$

The following formula is used to evaluate the order of convergence

$$cov.order = \begin{cases} log_2\left(\frac{\mathcal{L}_l(h,\Delta t_1)}{\mathcal{L}_l(h,\Delta t_2)}\right), & \text{in time,} \\ log_2\left(\frac{\mathcal{L}_l(h_1,\Delta t)}{\mathcal{L}_l(h_2,\Delta t)}\right), & \text{in space,} \end{cases} \tag{4.67}$$

where $l = 2$ or ∞.

Example 4.1. Numerical calculations are performed for an example on the assumption that the function $v(x,t) = (1+t^2+t^{3+\alpha})\sin(\pi x)$ is the exact solution of problem *(4.1)-(4.2)* with $b = 1$, $T = 1$, and coefficients $\mu_d = 1$, $q(t) = 1-\sin t$. This text example is corresponding to the smooth solution, so we have solved it using a uniform mesh.

Tables 4.1, 4.2, 4.3, and 4.4 represent the numerical results obtained for Example 4.1. Tables 4.1 and 4.2 show the $\mathcal{L}_\infty$-error, $\mathcal{L}_2$-error and the respective orders of convergence for multiple values of fractional order α with $N_x = 2000$. From these tables, it can be seen that as the partition number N_t increases, the errors decrease as expected. Also, these tables indicate that the order of convergence in the temporal direction is numerically calculated almost as $(2-\alpha)$, which is in agreement with Theorem 4.3. Table 4.3 display the $\mathcal{L}_\infty$-error and respective spatial orders of convergence that are evaluated for $N_t = 1000$, and different spatial mesh spacing h with $\alpha = 0.5$. Similarly, Table 4.4 shows the $\mathcal{L}_2$-error and the corresponding orders of convergence with $N_t = 4000$ and $\alpha = 0.8$. From Tables 4.3 and 4.4, we observe that the numerical results are similar for both schemes (marginally better for the present scheme).

In Figure 4.1, a comparison between the exact solution and the numerical solution of Example 4.1 is shown at different time levels when $\alpha = 0.8$ and $N_x = N_t = 100$. From the graph, we can observe that the numerical solution matches well with the exact solution. In a similar manner, Figure 4.2 represents the numerical solution of Example 4.1 for various fractional orders α at $x = 0.1$.

Example 4.2. Numerical calculations are performed for an example on the assumption that the function $v(x,t) = (t^\alpha + t^3)\sin x$ is the exact solution of problem *(4.1)-(4.2)* with $b = \pi$, $T = 1$, and coefficients $\mu_d = 1$, $q(t) = 1 - \sin t$. This test example is corresponding to the non-smooth solution, so we have solved it using the non-uniform mesh defined in *(4.4)*.

In the case of non-smooth solution the order of convergence in temporal direction is $N_t^{-\min\{2-\alpha,\theta\alpha\}}$. So, if we take $\theta = 1$, then we obtain the convergence order as α. If we choose $\theta = \left(\frac{2-\alpha}{2\alpha}\right)$, then we obtain the convergence order as $\left(\frac{2-\alpha}{2}\right)$, and if we take $\theta \geq \left(\frac{2-\alpha}{\alpha}\right)$, then we have the optimal order of convergence $(2-\alpha)$. So, for solving Example 4.2 we have considered $\theta = \left(\frac{2-\alpha}{\alpha}\right)$.

Tables 4.5, 4.6, 4.7 and 4.8 display the numerical results obtained for Example 4.2. Table 4.5 represents the $\mathcal{L}_\infty$-error and the respective order of convergence for multiple values of the fractional order α. The results of this table indicate that on a non-uniform mesh, the order of convergence in the temporal direction is numerically calculated as $N_t^{-(2-\alpha)}$, while on a uniform mesh, it gets reduced due to the singularity present in the derivative of the solution. Similarly, Table 4.6 represents $\mathcal{L}_2$-error and the respective order of convergence in temporal direction for multiple values of the fractional order α. The results obtained on both uniform and non-uniform meshes are compared in this Table, showing that the latter provides convergence order $N_t^{-(2-\alpha)}$ that validates the theoretical findings.

Tables 4.7 and 4.8 show that the $\mathcal{L}_\infty$-error and $\mathcal{L}_2$-error evaluated for $N_t = 4000$ and different spatial mesh spacing h with $\alpha = 0.3$ and $\alpha = 0.6$ respectively, decrease by decreasing the mesh spacing h. These tables also show that the convergence order

TABLE 4.1: (Example 4.1) $\mathcal{L}_\infty$-error and corresponding temporal order of convergence with $h = \frac{1}{2000}$.

N_t	10	20	40	80	160
$\alpha = 0.1$	3.6130e-04	1.0854e-04	3.1671e-05	8.8258e-06	2.1473e-06
		1.7350	1.7770	1.8434	2.0392
$\alpha = 0.2$	9.6852e-04	3.0566e-04	9.4224e-05	2.8357e-05	8.1730e-06
		1.6639	1.6978	1.7324	1.7948
$\alpha = 0.4$	3.5431e-03	1.2458e-03	4.2926e-04	1.4579e-04	4.8849e-05
		1.5079	1.5371	1.5580	1.5775
$\alpha = 0.6$	9.8524e-03	3.9060e-03	1.5212e-03	5.8606e-04	2.2416e-04
		1.3348	1.3605	1.3761	1.3865
$\alpha = 0.8$	2.4366e-02	1.0970e-02	4.8636e-03	2.1383e-03	9.3573e-04
		1.1513	1.1734	1.1855	1.1923
$\alpha = 0.9$	3.7217e-02	1.7877e-02	8.4686e-03	3.9824e-03	1.8654e-03
		1.0578	1.0779	1.0885	1.0941

in the spatial direction is two, and this is in agreement with the theoretical order of convergence. Moreover, from both these tables, we observe that the numerical results are similar for both schemes (marginally better for the present scheme).

Figure 4.3 represents the surface plots of the absolute error on both uniform and non-uniform meshes with $N_x = N_t = 60$ and $\alpha = 0.5$ for Example 4.2. It can be seen from this graph that towards the initial time, the error increases, and our method provides much better results on non-uniform meshes than on uniform ones. In Figure 4.4, a comparison between the exact solution and the numerical solution of Example 4.2 is shown at different time levels when $\alpha = 0.4$ and $N_x = N_t = 100$. From this graph, we can observe that the numerical solution matches well with the exact solution. In a similar manner Figure 4.5 represents the numerical solution of Example 4.2 for various fractional orders α at $x = 0.1$. We observe here that as the fractional order α decreases, the layer becomes sharper at starting time $t = 0$ in the solution.

TABLE 4.2: (Example 4.1) $\mathcal{L}_2$-error and corresponding temporal order of convergence with $h = \frac{1}{2000}$.

N_t	10	20	40	80	160
$\alpha = 0.1$	2.5548e-04	7.6750e-05	2.2395e-05	6.2408e-06	1.5184e-06
		1.7350	1.7770	1.8434	2.0392
$\alpha = 0.2$	6.8485e-04	2.1613e-04	6.6626e-05	2.0052e-05	5.7792e-06
		1.6639	1.6978	1.7324	1.7948
$\alpha = 0.4$	2.5053e-03	8.8091e-04	3.0354e-04	1.0309e-04	3.4541e-05
		1.5079	1.5371	1.5580	1.5775
$\alpha = 0.6$	6.9667e-03	2.7620e-03	1.0756e-03	4.1441e-04	1.5851e-04
		1.3348	1.3605	1.3761	1.3865
$\alpha = 0.8$	1.7229e-02	7.7568e-03	3.4391e-03	1.5120e-03	6.6166e-04
		1.1513	1.1734	1.1855	1.1923
$\alpha = 0.9$	2.6316e-02	1.2641e-02	5.9882e-03	2.8160e-03	1.3191e-03
		1.0578	1.0779	1.0885	1.0941

TABLE 4.3: (Example 4.1) $\mathcal{L}_\infty$-error and corresponding spatial order of convergence with $\alpha = 0.5$, $N_t = 1000$.

	Proposed work		Method in[103]	
N_x	$\mathcal{L}_\infty$-error	cov.order$_x$	$\mathcal{L}_\infty$-error	cov.order$_x$
2^3	3.3226e-02	-	3.3644e-02	-
2^4	8.3785e-03	1.9943	8.3785e-03	2.0056
2^5	2.0820e-03	2.0020	2.0975e-03	1.9980
2^6	5.1539e-04	2.0142	5.2947e-04	1.9860
2^7	1.2362e-04	2.0598	1.3760e-04	1.9441

TABLE 4.4: (Example 4.1) $\mathcal{L}_2$-error and corresponding spatial order of convergence with $\alpha = 0.8$, $N_t = 4000$.

	Proposed work		Method in[103]	
N_x	$\mathcal{L}_2$-error	cov.order$_x$	$\mathcal{L}_2$-error	cov.order$_x$
2^3	2.2849e-02	-	2.3141e-02	-
2^4	5.7267e-03	1.9964	5.7711e-03	2.0035
2^5	1.4227e-03	2.0091	1.4517e-03	1.9911
2^6	3.4527e-04	2.0428	3.7334e-04	1.9592
2^7	7.5822e-05	2.1870	1.0383e-04	1.8463

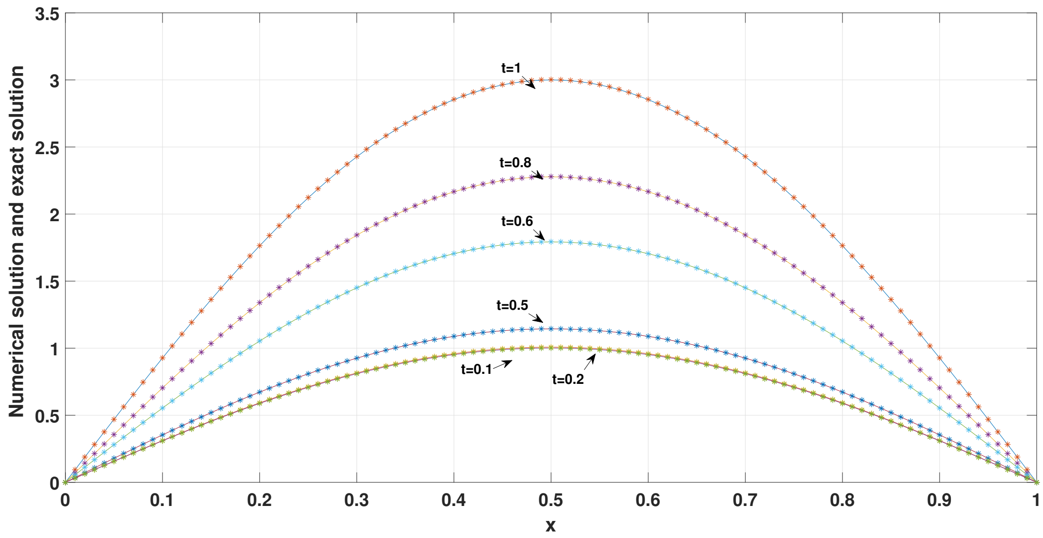

FIGURE 4.1: Numerical solution (starred line) and exact solution (solid line) of Example 4.1 with $\alpha = 0.8$ and $N_x = N_t = 100$ at different time levels t.

TABLE 4.5: (Example 4.2) $\mathcal{L}_\infty$-error and corresponding temporal order of convergence.

		Uniform mesh		Non-uniform mesh	
α	$N_x = N_t$	$\mathcal{L}_\infty$-error	cov.order$_t$	$\mathcal{L}_\infty$-error	cov.order$_t$
0.3	2^6	3.4921e-02		3.4958e-03	
	2^7	3.0265e-02	0.20644	1.2167e-03	1.5226
	2^8	2.6020e-02	0.21803	4.0890e-04	1.5732
	2^9	2.2196e-02	0.22933	1.3439e-04	1.6053
	2^{10}	1.8797e-02	0.23974	4.3748e-05	1.6191
0.6	2^6	1.4920e-02		4.5285e-03	
	2^7	1.0285e-02	0.53674	1.7910e-03	1.3383
	2^8	6.9937e-03	0.55642	6.9722e-04	1.3611
	2^9	4.7098e-03	0.57041	2.6878e-04	1.3752
	2^{10}	3.1504e-03	0.58010	1.0298e-04	1.3840
0.9	2^6	8.5141e-03		1.0276e-02	
	2^7	3.9694e-03	1.1009	4.8262e-03	1.0903
	2^8	1.8403e-03	1.1090	2.2567e-03	1.0966
	2^9	8.5019e-04	1.1141	1.0529e-03	1.0999
	2^{10}	3.9180e-04	1.1177	4.9066e-04	1.1015

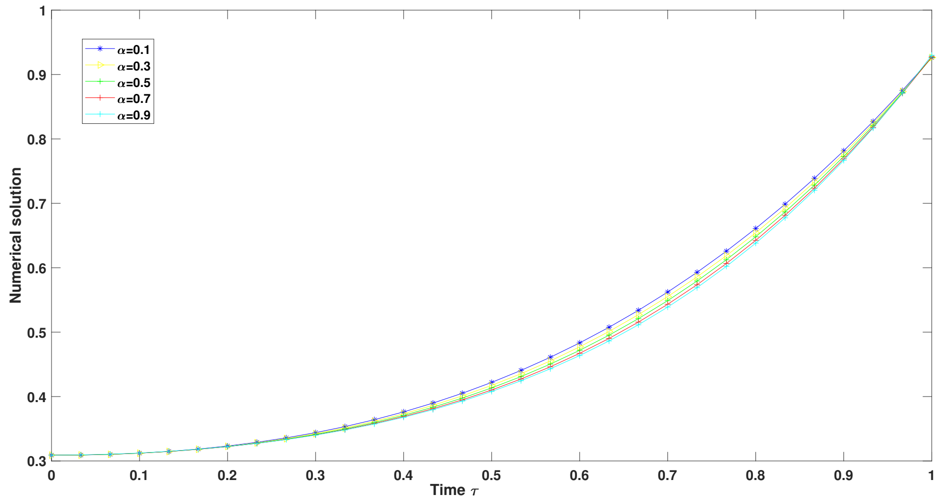

FIGURE 4.2: Numerical solution of Example 4.1 for different α at $x = 0.1$.

TABLE 4.6: (Example 4.2) $\mathcal{L}_2$-error and corresponding temporal order of convergence.

		Uniform mesh		Non-uniform mesh	
α	$N_x = N_t$	$\mathcal{L}_2$-error	cov.order$_t$	$\mathcal{L}_2$-error	cov.order$_t$
0.3	2^6	4.3766e-02		4.3814e-03	
	2^7	3.7931e-02	0.20644	1.5249e-03	1.5226
	2^8	3.2611e-02	0.21803	5.1248e-04	1.5732
	2^9	2.7818e-02	0.22933	1.6844e-04	1.6053
	2^{10}	2.3559e-02	0.23974	5.4862e-05	1.6183
0.6	2^6	1.8700e-02		5.6756e-03	
	2^7	1.2890e-02	0.53674	2.2447e-03	1.3383
	2^8	8.7653e-03	0.55642	8.7383e-04	1.3611
	2^9	5.9028e-03	0.57041	3.3687e-04	1.3752
	2^{10}	3.9485e-03	0.58010	1.2907e-04	1.3840
0.9	2^6	1.0671e-02		1.2879e-02	
	2^7	4.9749e-03	1.1009	6.0487e-03	1.0903
	2^8	2.3064e-03	1.1090	2.8284e-03	1.0966
	2^9	1.0656e-03	1.1141	1.3196e-03	1.0999
	2^{10}	4.9105e-04	1.1177	6.1495e-04	1.1015

TABLE 4.7: (Example 4.2) $\mathcal{L}_\infty$-error and corresponding spatial order of convergence with $\alpha = 0.3$, $N_t = 4000$.

	Proposed work		Method in[103]	
N_x	$\mathcal{L}_\infty$-error	cov.order$_x$	$\mathcal{L}_\infty$-error	cov.order$_x$
2^3	1.3521e-02	-	1.3546e-02	-
2^4	3.3735e-03	2.0029	3.3935e-03	1.9970
2^5	8.3599e-04	2.0127	8.5577e-04	1.9875
2^6	2.0159e-04	2.0521	2.2135e-04	1.9509
2^7	4.3312e-05	2.2186	5.8081e-05	1.9302

TABLE 4.8: (Example 4.2) $\mathcal{L}_2$-error and corresponding spatial order of convergence with $\alpha = 0.6$, $N_t = 4000$.

	Proposed work		Method in[103]	
N_x	$\mathcal{L}_2$-error	cov.order$_x$	$\mathcal{L}_2$-error	cov.order$_x$
2^3	9.2952e-03	-	9.3135e-03	-
2^4	2.3111e-03	2.0079	2.3413e-03	1.9920
2^5	5.6608e-04	2.0295	5.9704e-04	1.9714
2^6	1.2989e-04	2.1237	1.5758e-04	1.9217
2^7	2.0844e-05	2.6396	4.2217e-05	1.9002

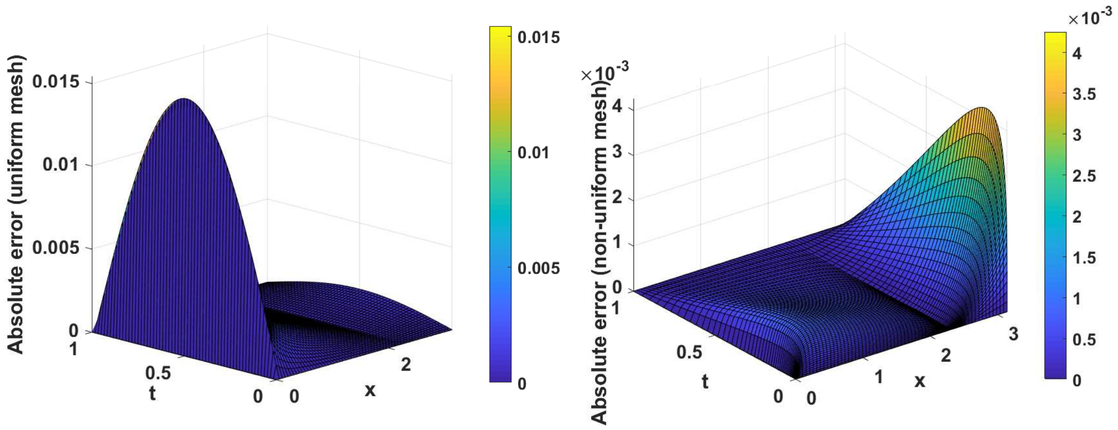

(a) On uniform mesh (b) On non-uniform mesh

FIGURE 4.3: surface plots of absolute error of Example 4.2 with $N_x = N_t = 60$ and $\alpha = 0.5$.

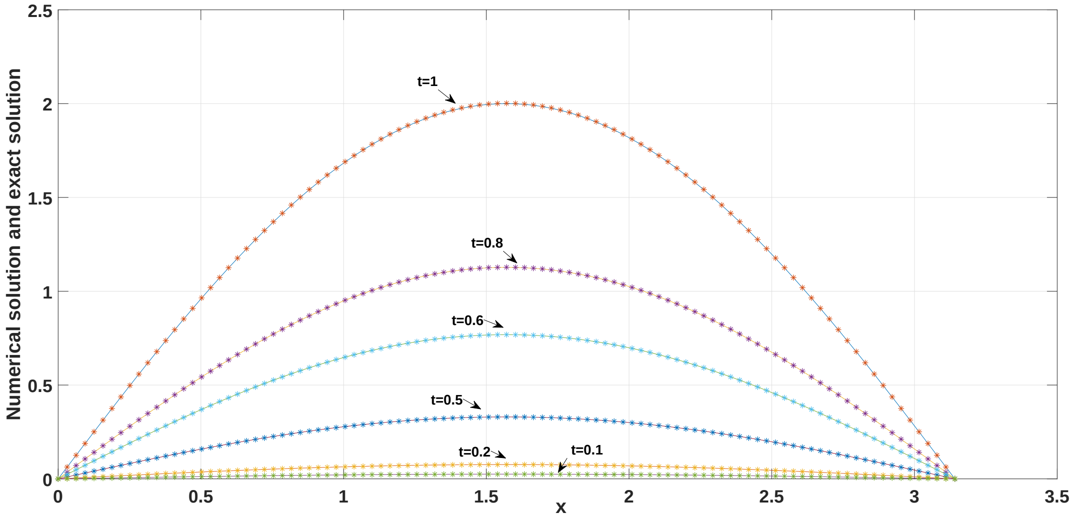

FIGURE 4.4: Numerical solution (starred line) and exact solution (solid line) of Example 4.2 with $\alpha = 0.4$ and $N_x = N_t = 100$ at different time levels t.

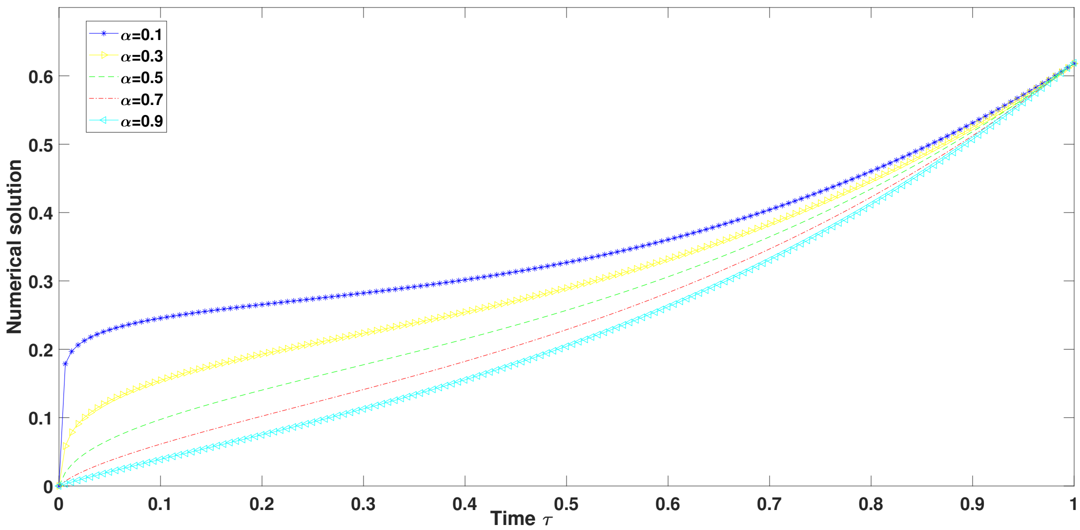

FIGURE 4.5: Numerical solution of Example 4.2 for different α at $x = 0.1$.

4.4.1 Applications

Here, we provide applications of the considered time-fractional reaction-diffusion model.

- Through heterogeneous media, we can summarize tracer transport by using the following time-fractional convection-diffusion model [106]:

$$ {}_0^C D_t^{\alpha(t)} \vartheta(x,t) - \mu_d \frac{\partial^2 \vartheta(x,t)}{\partial x^2} + a \frac{\partial \vartheta(x,t)}{\partial x} = 0, \quad (x,t) \in (0,b) \times (0,T], \quad (4.68) $$

  where μ_d is the diffusion coefficient, a is the mean flow velocity and $\alpha(t) \in (0,1)$ is the temporal fractional order of differentiation which may be a variable or a constant. As we know the transient dispersion generalizes the transient anomalous dispersion. In [106] it is stated that the model (4.68) can also summarize a transient sub-dispersion. Thus, by taking $\alpha(t) = \alpha$ and using the following exponential transformation

$$ \vartheta(x,t) = e^{(ax/2\mu_d)} v(x,t) \quad (4.69) $$

  in equation (4.68), we can get the following time-fractional reaction-diffusion model

$$ {}_0^C D_t^{\alpha} v(x,t) - \mu_d \frac{\partial^2 v(x,t)}{\partial x^2} + a v(x,t) = 0, \quad (x,t) \in (0,b) \times (0,T], \quad (4.70) $$

  where $0 < \alpha < 1$. The model problem (4.70) is a particular case of the time-fractional reaction-diffusion model (4.1) with variable coefficients. Therefore, we can easily solve the model problem (4.70) by the proposed numerical method (4.16)-(4.17) to describe the anomalous uranine transport in a pseudo one-dimensional fractured porous medium.

- To model gas transport through heterogeneous soil and gas reservoirs, Chang et al. [16] used the following time fractional convection-diffusion equation:

$$ {}_0^C D_t^\alpha \vartheta(x,t) = -a\frac{\partial \vartheta(x,t)}{\partial x} + \mu_d \frac{\partial^2 \vartheta(x,t)}{\partial x^2}, \quad 0 < \alpha < 1, \tag{4.71} $$

where ϑ is is the gas concentration, a is the average pore velocity and μ_d is the diffusion coefficient. In [16], the authors first considered the integer order convection-diffusion model, and since fractional derivatives can reflect the history dependence and path of the mass particles, therefore to model gas transport in natural media without mass insertion, they generalized it to the fractional order model.

Further, we can use the exponential transformation given in equation (4.69) and obtain the time-fractional reaction-diffusion model (4.70), which can be solved using the proposed numerical method (4.16)-(4.17) to model gas transport through heterogeneous soil and gas reservoirs.

4.5 Conclusion

The present numerical scheme with the L1 approximation method in time discretization on a non-uniform graded mesh and the cubic spline approximation method on a uniform mesh in spatial discretization is a satisfactory way of solving the time-fractional reaction-diffusion equation. The cause behind the use of a non-uniform graded mesh is that for the typical (non-smooth) solution, we are required the grading of the mesh in a way that the mesh should be finer near $t = 0$ for handling the singular behaviour of the solution near $t = 0$. We have observed that a non-uniform mesh used for the typical (non-smooth) solution gave good results than a uniform mesh. The proposed method is shown to be unconditionally stable. In addition, convergence analysis is given separately for both smooth and non-smooth solutions, and it is shown that the proposed method gives optimal convergence results for both smooth and non-smooth solutions. The robustness and accuracy of the proposed method are demonstrated with the help of two test examples. The obtained numerical results show that the method accurately approximates the problem and the results are in line with the theoretical analysis.